The Breast 53 (2020) 102–110

Contents lists available at ScienceDirect

The Breast

journal homepage: www.elsevier.com/brst

Original article

Sequential immunohistochemistry and virtual image reconstruction using a single slide for quantitative KI67 measurement in breast cancer

Garazi Serna [a], Sara Simonetti [a], Roberta Fasani [a], Francesca Pagliuca [b], Xavier Guardia [a], Paqui Gallego [a], Jose Jimenez [a], Vicente Peg [c], Cristina Saura [d], Serenella Eppenberger-Castori [e], Santiago Ramon y Cajal [c], Luigi Terracciano [e], Paolo Nuciforo [a, *]

[a] Molecular Oncology Group, Vall D'Hebron Institute of Oncology, Barcelona, Spain
[b] University of Naples Federico II, Department of Advanced Biomedical Sciences, Pathology Section, Naples, Italy
[c] Department of Pathology, Vall D'Hebron University Hospital, Barcelona, Spain
[d] Breast Cancer and Melanoma Group, Vall D'Hebron Institute of Oncology, Barcelona, Spain
[e] Institute of Pathology, University Hospital Basel, Basel, Switzerland

ARTICLE INFO

Article history:
Received 4 April 2020
Received in revised form
12 June 2020
Accepted 8 July 2020
Available online 13 July 2020

Keywords:
Ki67 quantification
Breast cancer
Prognosis
Sequential immunohistochemistry
Digital image analysis

ABSTRACT

Objective: Ki67 is a prognostic and predictive marker in breast cancer (BC). However, manual scoring (MS) by visual assessment suffers from high inter-observer variability which limits its clinical use. Here, we developed a new digital image analysis (DIA) workflow, named KiQuant for automated scoring of Ki67 and investigated its equivalence with standard pathologist's assessment.

Methods: Sequential immunohistochemistry of Ki67 and cytokeratin, for precise tumor cell recognition, were performed in the same section of 5 tissue microarrays containing 329 tumor cores from different breast cancer subtypes. Slides were digitalized and subjected to DIA and MS for Ki67 assessment. The intraclass correlation coefficient (ICC) and Bland-Altman plot were used to evaluate inter-observer reproducibility. The Kaplan-Meier analysis was used to determine the prognostic potential.

Results: KiQuant showed an excellent correlation with MS (ICC:0.905,95%CI:0.878–0.926) with satisfactory inter-run (ICC:0.917,95%CI:0.884–0.942) and inter-antibody reproducibilities (ICC:0.886,95% CI:0.820–0.929). The distance between KiQuant and MS increased with the magnitude of Ki67 measurement and positively correlated with analyzed tumor area and breast cancer subtype. Agreement rates between KiQuant and MS within the clinically relevant 14% and 30% cut-off points ranged from 33% to 44% with modest interobserver reproducibility below the 20% cut-off (0.606, 95%CI:0.467–0.727). High Ki67 by KiQuant correlated with worse outcome in all BC and in the luminal subtype ($P = 0.028$ and $P = 0.043$, respectively). For MS, the association with survival was significant only in 1 out of 3 observers.

Conclusions: KiQuant represents an easy and accurate methodology for Ki67 measurement providing a step toward utilizing Ki67 in the clinical setting.

1. Introduction

Ki67 is a nuclear protein expressed throughout all the phases of the cell cycle from G1 to M-phase [1]. Due to its association with cellular proliferation, Ki67 detection by immunohistochemistry (IHC) has emerged as a useful and inexpensive tool to assess the proliferation index of a tumor. Many studies have shown prognostic and predictive values of Ki67 in a wide range of malignancies [2] [–] [9]. In particular, in breast cancer (BC), Ki67 has been successfully used not only for classification and risk assessment purposes but also to decide therapeutic endpoints in the context of neoadjuvant settings [10] [–] [13].

The promise of Ki67 as a biomarker is affected by technical and

* Corresponding author. Molecular Oncology Group, Vall d'Hebron University Hospital, Vall d'Hebron Institute of Oncology (VHIO) C/ Natzaret, 115-117, 08035, Barcelona, Spain.
E-mail address: pnuciforo@vhio.net (P. Nuciforo).

https://doi.org/10.1016/j.breast.2020.07.002

scoring reproducibility issues, which make it not ready for clinical use. Despite the efforts of the International Ki67 in Breast Cancer Working Group (IKWG) to standardize the preanalytical, analytical, interpretation, and data analysis steps, variations in protocols and scoring methodologies across laboratories remain large contributors to assay variability [14,15]. Manual counting provides better interobserver reproducibility as compared to visual estimation [16]. However, as scoring the whole section seems impractical, the location and extent of the area that should be scored are controversial and subject to observer's interpretation [17,18]. As a consequence, despite different Ki67 thresholds to define luminal A vs luminal B tumors (14%, 20%, laboratory median values [19] [–] [21]) have been proposed, no absolute standard methodology and cut-off point have been defined so far. In this context, the use of multigene tests [22–24] and digital image analysis (DIA) [25–32] may be valuable, especially across intermediate Ki67 levels where there is high uncertainty.

While computer-assisted methods are expected to provide a more accurate Ki67 assessment, these approaches either rely on significant pathologist's intervention for the area of interest selection or use unique and sophisticated cell segmentation and classification algorithms that require extensive supervised learning.

In this study, we describe a novel methodology for automatic scoring of Ki67 which relies on sequential IHC of Ki67 and cytokeratin using a single slide, followed by virtual image reconstruction for DIA. The use of a cytokeratin mask allows for the precise definition of the region of interest and limits pathologist's intervention. The methodology accuracy was compared with manual scoring (MS) determined by multiple observers to demonstrate equivalence or superiority. Finally, the outcome prediction potential of our method was investigated.

2. Material and methods

2.1. Patients and samples

Clinicopathological features of study cohorts are shown in Table 1. A total of 186 patients from 2 different cohorts was used in this study. Cohort 1 was composed of 99 patients with BC of different subtypes [hormone receptor-positive (HR+), HER2-positive (HER2+), and triple-negative (TN)] retrieved from the Pathology Department of the Vall d'Hebron University Hospital (Barcelona, Spain). No survival data were available for this cohort. Cohort 2 comprised an independent set of 87 BCE patients selected from the archives of the Pathology Department of the University Basel Hospital (Basel, Switzerland), with 58 months median follow up for overall survival (OS).

From the surgical specimens of primary BC of each patient, a representative paraffin-embedded tumor tissue block was selected and five tissue microarrays (TMAs), containing representative BC tissue cores of 1.5 mm, were built. For cohort 1, four TMAs were constructed, containing between 2 and 3 cores of 1.5 mm for each tumor, with a total of 242 cores. Cohort 2 BCE cancer specimens were arrayed in one TMA built using one representative core for each tumor sample (87 cores of 1.5 mm).

The protocol of this study was approved by the Vall d'Hebron University Hospital Ethical Committee (PR(AG)76/2018) and all methods were performed in accordance with relevant guidelines and regulations.

2.2. Immunohistochemistry

The complete sequential IHC and image analysis workflow used in this study (named KiQuant) is illustrated in Fig. 1A. Briefly, after deparaffinization and antigen retrieval (CC1, 64 min at 95 °C), one single slide of each TMA was first stained with a standard anti-Ki67 primary antibody (clone 30–9, prediluted, #790–4286, Ventana, Tucson AZ) for 64 min at 37 °C on an automated staining system (Discovery Ultra, Ventana, Tucson AZ). Antibody binding was amplified with an anti-Rb HRP biotin-free detection system (#760–4315, Ventana, Tucson AZ) ,visualized using 3-amino-9-ethylcarbazole (Mono AEC/Plus, #K050, PALEX), an alcohol soluble substrate that results in red staining, and counterstained with hematoxylin. The slides were mounted and digitalized at 20x using a slide scanner (NanoZoomer 2.0HT, Hamamatsu Photonics, Japan). Following digitalization, the coverslip was removed before destaining using ethanol as previously described (Tsujikawa, Cell Reports 2017; Glass, J Histochem Cytochem 2009). The destained slides were then subjected to an additional antigen retrieval step (CC2, 8 min at 100 °C) to completely strip the first primary antibody (anti-Ki67) before the second staining cycle with another antigen retrieval (CC1, 48 min at 95 °C) was started. Then, the anti-Pan-Keratin primary antibody (clone AE1/AE3/PCK26, prediluted, #760–2135, Ventana, Tucson AZ) was applied for 40 min at 36 °C. Antibody binding was amplified with an anti-MS HRP biotin-free detection system (#760–4313, Ventana, Tucson AZ). For reproducibility analyses, a second anti-Ki67 antibody was also used (clone MIB-1, #M7240, DAKO/Agilent, Santa Clara, CA) for IHC in a non-consecutive slide from a TMA of cohort 1.

Table 1
Clinicopathologic characteristcs of study cohorts.

	Cohort 1		Cohort 2	
	N	%	*N*	%
Patients	99	100	87	100
Diagnosis				
Invasive ductal carcinoma	78	78.8	61	70.1
Invasive lobular carcinoma	12	12.1	14	16.1
Mixed ductal-lobular carcinoma	0	0.0	10	11.5
Medullary carcinoma	1	1.0	1	1.1
Mucinous carcinoma	3	3.0	1	1.1
Metaplastic carcinoma	5	5.1	0	0.0
Grade				
I	1	1.0	8	9.2
II	39	39.4	37	42.5
III	54	54.5	42	48.3
NA	5	5.1	0	0.0
pT				
T1	17	17.2	32	36.8
T2	56	56.6	41	47.1
T3	15	15.2	6	6.9
T4	1	1.0	8	9.2
NA	10	10.1	0	0.0
pN				
Negative	44	44.4	39	44.8
Positive	50	50.5	43	49.4
NA	5	5.1	5	5.7
pM				
0	99	100	83	95.4
1	0	0,0	4	4.6
Subtype				
HER2+	23	23.2	9	10.3
HR+	39	39.4	62	71.3
TNBC	37	37.4	16	18.4

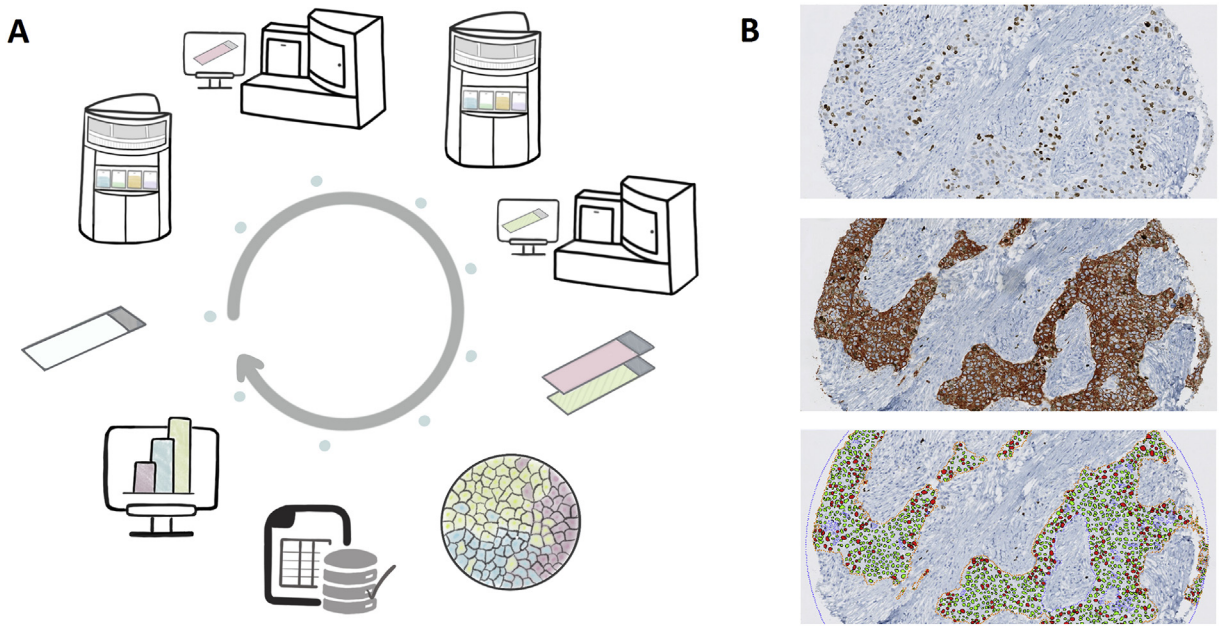

Fig. 1. KiQuant workflow. A) This workflow uses sequential Ki67 and cytokeratin (for precise automatic tumor cells recognition) immunohistochemistry staining on the same tissue section. The steps are: staining of the slide with the first primary antibody anti-Ki67, digitalization of the slide after the first staining, coverslip removal and staining of the slide with the second primary antibody anti-Pan-Keratin, digitalization of the slide after the second staining, image alignment, image analysis, quality check, and data report. B) A representative example of a tumor core sequentially stained with Ki67 (top) and Pan-Keratin (middle). In the virtual digital image (bottom), Pan-Keratin-positive brown areas are used to automatically mark the region of interest (dotted orange line). Green and red cells represent Ki67-negative and -positive nuclei, respectively. Ki67-labelled stromal cells not stained by the Pan-Keratin antibody are excluded from the analysis.

2.3. Digital image analysis (DIA)

To analyze the images, we created an algorithm using the Author® module of VISIOPHARM® (VIS) Image Analysis Software (Visiopharm Integrator System version 2019.January 02, 6005, Visiopharm, Denmark). Both Ki67 and cytokeratin stained digitalized slides were automatically registered, to fuse the information into a single virtual digital image (VDI), using the Tissuealign® module of VIS. Cytokeratin stained images were used to classify tumor and stromal areas within each core. A color deconvolution algorithm enhanced tumoral areas that were extracted using a pixel intensity threshold algorithm. Cytokeratin-based segmentations were transferred to the registered Ki67 image. Cells within the cytokeratin mask were classified into Ki67 positive or negative using a cell classification method based on form and size, and a pixel-color intensity threshold method, which considered only KI67 nuclear staining (algorithms specifications in Supplementary Table 1 and algorithms in Supplementary Material).

Each core on the TMA slides was separately analyzed by locating the tissue, using an automatic thresholding approach, and extracting the area of interest to create separate images. Cytokeratin-positive non cancer areas (such as ductal carcinomas in situ, necrosis or normal ducts) were manually excluded before data extraction. Final results are reported as the cell density, i.e. the total number of cells within the tumor area defined by the mask, number of positive and number of negative cell nuclei, as well as the percentage of positive cells within the corresponding core.

The application was trained by a biotechnologist, expert in image analysis, to identify positive and negative Ki67 cells within the tumor mask in the VDI (Fig. 1B). After setting the optimal conditions, the methodology was evaluated in samples from cohort 1 and validated on an independent group with follow up data. The framework performance was compared to the results obtained by manual scoring (MS) of three expert board-certified pathologists. MS LI is defined as the ratio between the number of KI67-positive tumor cells and the total number of tumor cells, using either counting or estimation approaches[14] (Supplementary Table 2). Individual images were manually reviewed to exclude non-evaluable cores (n = 24, unpaired cores, cores containing only normal tissue, folded cores or cores without cytokeratin staining).

Method reproducibility was investigated by analyzing KiQuant results obtained by a) staining and analysis of two TMAs (TMA2 and TMA3) during two non-consecutive days (inter-run reproducibility), and b) by staining of two non-consecutive sections of one TMA (TMA2) with two different commonly used anti-Ki67 primary antibodies [inter-antibody reproducibility, clone 30–9 from Ventana (Tucson, AZ, USA) and clone MIB1 from DAKO/Agilent (Santa Clara, CA, USA)].

2.4. Statistical analysis

Agreement between KiQuant and MS was calculated using intraclass correlation coefficient (ICC) and Bland-Altman (BA) plot. We considered ICC values from 0.4 to 0.6 as moderate reliability, from 0.61 to 0.8 as good reliability, and greater than 0.8 as excellent reliability [33]. Spearman rank correlation coefficient and Kruskal-Wallis nonparametric test were used to determine the relationship of the difference between KiQuant and MS scoring with analyzed tumor area and BC subtypes, respectively. Overall survival was modeled using the Kaplan-Meier curves, and the significance of differences between these curves was determined using the log-rank test. Statistical analysis, data preparation, and figures were carried out with R-commander (v.1.9–5) and SPSS software (v.25.0; IBM (Armonk, NY, USA).

3. Results

3.1. Correlation between KiQuant and MS

KiQuant was compared with a reference standard Ki67 LI MS which was determined as the average Ki67 LI between two board-certified pathologists scoring 218 cores of cohort 1 using the counting method [14]. Correlation between KiQuant and MS was excellent (ICC: 0.905, 95% CI: 0.878–0.926). KiQuant returned systematically lower Ki67 LI results compared to MS (mean, 16.6% vs 21.7%, respectively). The correlation was better in HR+ (ICC: 0.934, 95% CI: 0.905–0.955) than in TNBC (ICC: 0.894, 95% CI: 0.835–0.933) and HER2+ (ICC: 0.862, 95% CI: 0.758–0.923) (Fig. 2A). BA plot revealed a significant proportional bias (regression analysis, $P < 0.0001$) by showing that the distance between KiQuant and MS increased with the magnitude of Ki67 measurement (Fig. 2B). The difference between KiQuant and MS correlated with the analyzed tumor area (Spearman's rho = 0.455, $P < 0.0001$), BC histology (mean difference, IDC = 5.4; ILC = 1.4; Medullary = 23.85; Metaplastic = 7.7; Mucinous = 0.6; Kruskal-Wallis test $P = 0.001$, Supplementary Figure S1) and subtype (mean difference, HER2+ = 7.4; TNBC = 6.3; HR+ = 3.1; Kruskal-Wallis test $P = 0.001$). Thirteen cores (6%) from 9 patients showed a difference between KiQuant and MS KI67 LI outside the limits of agreement (Supplementary Table 3).

3.2. Concordance of KiQuant and MS across different observers in luminal BC

Three different pathologists scored 100 cores of luminal (HR+) BC and individual observer MS were compared between each other and with KiQuant results (Fig. 3, Supplementary Table 4). Overall, the inter-pathologist concordance was very high (ICC: 0.932, 95% CI: 0.905–0.952). The agreement between KiQuant and each individual observer was excellent for all observers (OBS1 ICC: 0.877, 95% CI: 0.822–0.915; OBS2 ICC: 0.870, 95% CI: 0.810–0.911; OBS3 ICC: 0.842, 95% CI: 0.774–0.891). Then, we determined the agreement between KiQuant and individual MS across different Ki67 LI cut-offs. The highest concordance rates (ranging from 84% to 100%, depending on the observer) were found below the 2.7% and above the 40% cut-offs, whereas the lowest (ranging from 71% to 90%) were observed within 14% and 30% cut-offs (Supplementary table 4). At the clinically relevant cut-off of 20% defined by St Gallen criteria [20], concordance between KiQuant and MS ranged from 71% to 86%, depending on the observer. Inter-observer concordance was lower below the 20% (ICC: 0.606, 95% CI: 0.467–0.727) as compared to equal or above the 20% (ICC: 0.937, 95% CI: 0.893–0.965) cut-point defined by KiQuant.

3.3. KiQuant reproducibility

KiQuant inter-run correlation (n = 120 cores, ICC: 0.917, 95% CI: 0.884–0.942), and inter-antibody reproducibility (n = 64 evaluable cores, ICC: 0.886, 95% CI: 0.820–0.929) were excellent (Supplementary Figure S2).

3.4. Prognostic potential of Ki67 LI as determined by KiQuant and MS

To test the outcome prediction potential of KiQuant, we used an independent cohort of 87 breast invasive carcinomas with available outcome data (Table 1). The analysis was performed using the KiQuant workflow and obtained results were compared with the reference MS LI determined by 3 independent observers. Median Ki67 LI were used as cut-points. Patients with high Ki67 LI by KiQuant had shorted overall survival (all: log-rank, $P = 0.028$; HR+/HER2-: log-rank, $P = 0.043$). For MS LI, the association was statistically significant only in 1 out of 3 observers (Fig. 4, Supplementary

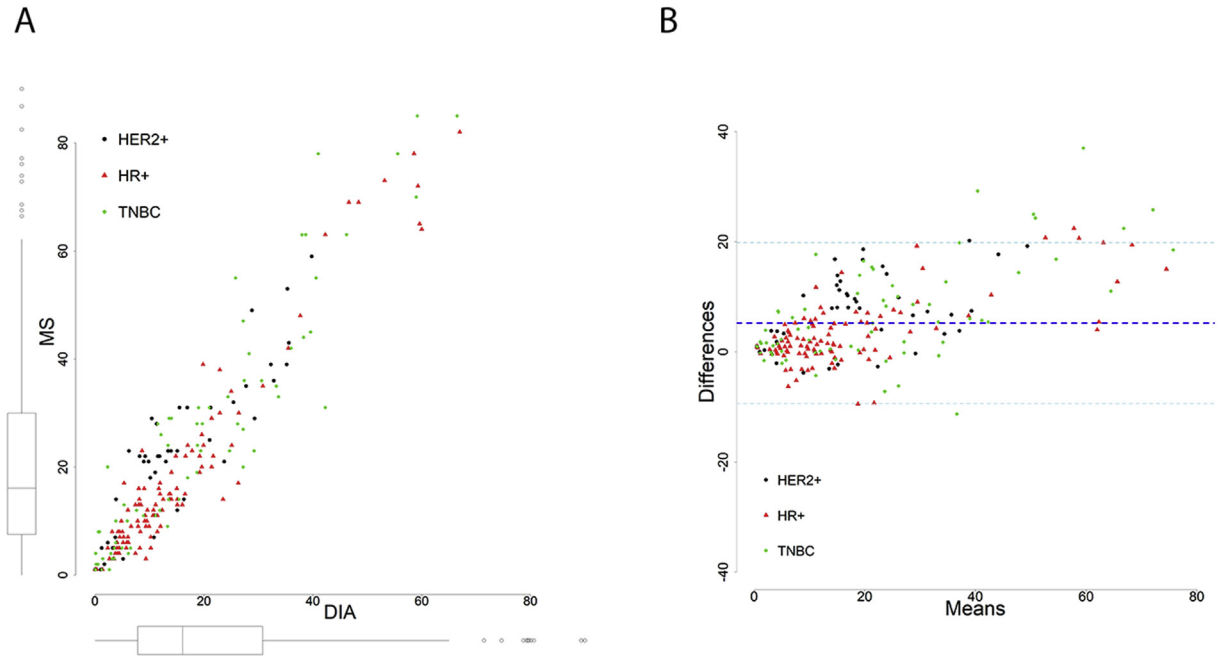

Fig. 2. A) Comparison of manual scoring (MS, y-axis) and KiQuant (DIA, x-axis) in breast cancer. The scattered plots are based on 218 evaluable cores from cohort 1. The breast cancer subtype is indicated in the legend of the top of the plots. Box plots of MS and KiQuant data are shown in the y-axis and x-axis, respectively. **B)** Bland-Altman plot of agreement between Ki67 labeling index (LI) by MS and KiQuant. In the x-axis, the average Ki67 LI between the two assessment methodologies is shown. The y-axis represents the difference between Ki67 LI scored by manual scoring and digital image analysis. The dotted blue line shows the average difference between the two assessments (4.95). The upper (19.51) and lower (−9.60) limits of agreement are indicated by the dotted light-blue lines.

CORE ID	OBS1	OBS2	OBS3	MS	KiQuant	KI67 range	% agreem KiQuant vs MS	ICC OBS
1	1	1	0	1	0	0-2.6%	100%	.606 (95% CI: 0.467-0.727)
2	1	1	0	1	0			
3	1	1	0	1	1			
4	2	5	2	3	4	2.7-13%	71%	
5	5	8	7	7	4			
6	5	8	5	6	4			
7	7	10	6	8	5			
8	15	7	22	15	5			
9	3		3	3	5			
10	7	5	6	6	5			
11	7	5	15	9	5			
12	5	5	5	5	5			
13	5	12	8	8	5			
14	5	7	5	6	6			
15	5	8	4	6	6			
16	7	5	10	7	6			
17	10	5	16	10	6			
18	7	10	6	8	6			
19	10		18	14	6			
20	10	5	20	12	7			
21	7	5	10	7	7			
22	10	15	15	13	7			
23	7	5	10	7	7			
24	3	5	3,4	4	7			
25	7		10	9	8			
26	12	5	24	14	8			
27	7	10	8	8	9			
28	10	3	12	8	9			
29		20	15	18	9			
30	7	15	20	14	9			
31	10	5	15	10	10			
32	10	15	23	16	10			
33	15		12	14	10			
34	15	5	42	21	11			
35	20	15	25	20	11			
36	15	8	19	14	11			
37	7	5	8	7	11			
38	12	10	11	11	11			
39	12	12	10	11	12			
40	25	10	28	21	12			
41	15	10	12	12	12			
42	15	10	25	17	14	14-29%	33%	
43	15		27	21	14			
44	20	10	27	19	14			
45	35	15	32	27	14			
46	17	20	15	17	14			
47	20	10	32	21	14			
48	7	5	10	7	14			
49	10	5	10	8	15			
50	15	5	25	15	15			
51	12	7	7	9	15			
52	10	5	15	10	16			
53	15	10	25	17	16			
54	30	20	32	27	16			
55	10	10	15	12	16			
56	15	15	25	18	17			
57	20	15	30	22	17			
58	25	10	25	20	17			
59	15	8	15	13	17			
60	12	10	16	13	17			
61	30	20	42	31	18			
62	10	10	12	11	18			
63	15	5	26	15	18			
64	20		50	35	19			
65	15	10	20	15	19			
66	25	15	28	23	20	20%-29%	42%	.937 (95% CI: 0.893-0.965)
67	20	10	35	22	20			
68	35	40	40	38	21			
69	35	15	50	33	21			
70	20	10	30	20	21			
71	15	8	20	14	22			
72	15	25	18	19	22			
73	25	50	42	39	23			
74	30	20	40	30	23			
75	30	15	33	26	24			
76	20	10	55	28	24			
77	12	15	27	18	24			
78	35	15	30	27	24			
79	30	20	41	30	25			
80	15	15	28	19	25			
81	35	10	41	29	26			
82	30	20	45	32	27			
83	20	20	20	20	28			
84	45	40	54	46	28			
85	35	20	30	28	30	30%-100%	75%	
86	25	20	40	28	30			
87	25	20	30	25	33			
88	50	35	51	45	36			
89	35	15	40	30	38			
90	30	20	40	30	43			
91	25	15	30	23	45			
92	75	60	70	68	51			
93	85	70	97	84	51			
94	90	80	90	87	51			
95	75	60	95	77	52			
96	95	80	90	88	57			
97	95	80	98	91	61			
98	90	85	95	90	71			
99	95	80	95	90	79			
100	95	90	98	94	93			

Fig. 3. Heat map of Ki67 scores. Rows represent cases and columns represent observers. Cases are ordered in ascending order by KiQuant values. Blue color gradients indicate Ki67 score ranges (0–2.6%, 2.7–13%, 14–19%, 20–29%, 30–100%). The percentage of agreement between KiQuant and MS (manual scoring represented by the average value among the three observers) is indicated for each Ki67 score range. Intraclass correlation coefficient (ICC) among the three observers and 95% confidence interval (CI) is shown for each Ki67 score range.

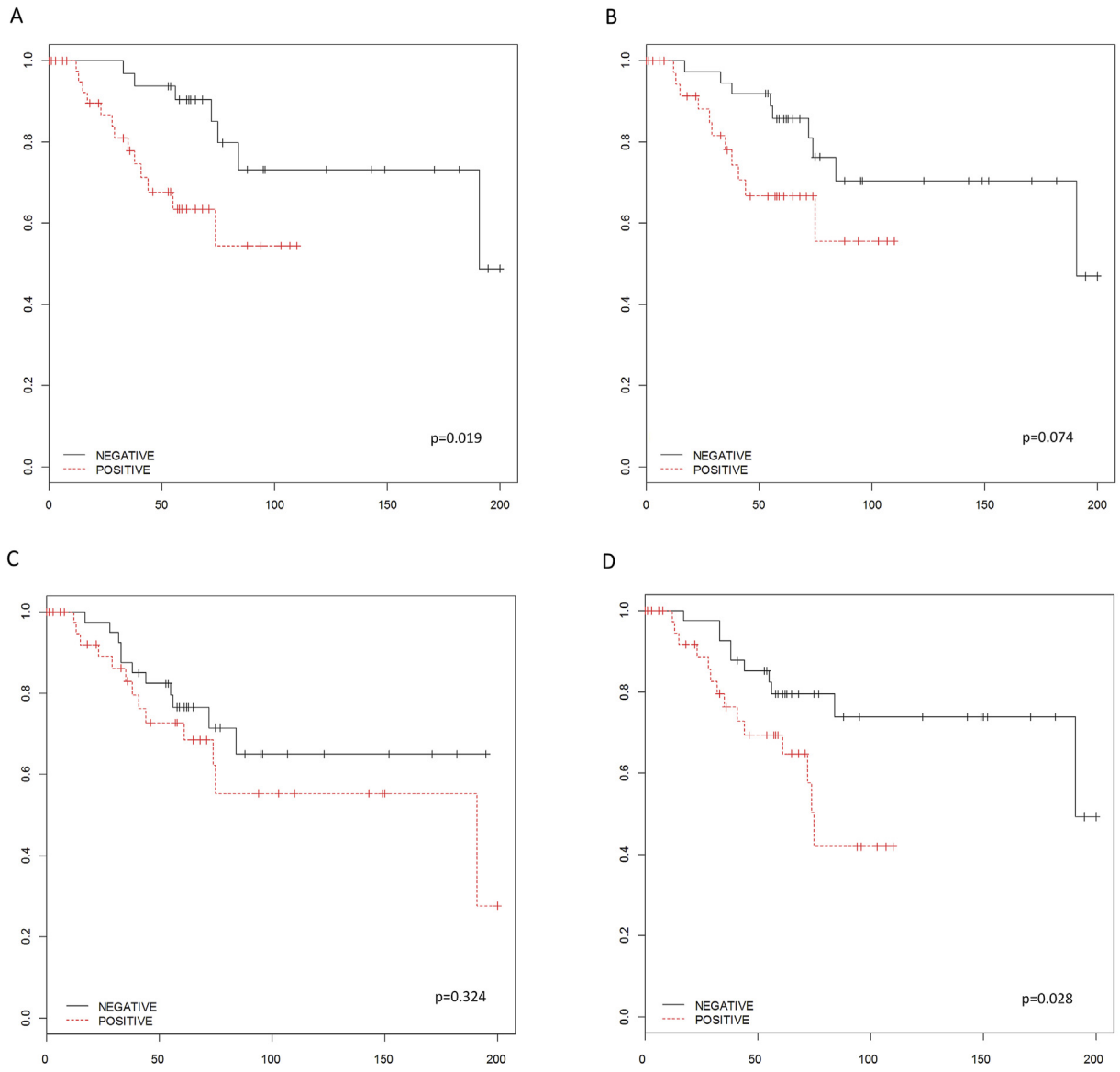

Fig. 4. Kaplan-Meier curves of overall survival according to Ki67 scores determined by three different observers (A, B and C) and KiQuant (D). Negative (black) and positive (red) lines correspond to patients having a Ki67 LI less or above the median Ki67 value, respectively. *P*-values are from the Log-rank test.

Figure S3).

4. Discussion

Ki67 is a useful biomarker for risk stratification, helps to differentiate luminal A- and B-type tumors, and to decide end-of-neoadjuvant-treatment endopoint in clinical trials, thus providing predictive and prognostic information in BC [19,34–38]. However, its implementation in the clinical setting has been hampered by the high technical and interpretation variability, and most significantly, the poor reproducibility across operators and laboratories [15,39]. The European Society for Medical Oncology (ESMO) and the American Society of Clinical Oncology (ASCO) have concluded that Ki67 would be a useful clinical tool if standardized [40,41]. Meanwhile, the use of multigene predictors has given clinicians a more accurate methodology for risk stratification [22–24]. DIA platforms using machine-learning (ML) methods have been proposed as automated systems for Ki67 LI scoring. A recent study comparing different software packages showed an excellent agreement across the different DIA platforms (ICC: 0.933) which suggests that DIA can be standardized to give highly reproducible, platform-independent Ki67 LI automatic evaluation ([42–44].

In this study, we proposed a fairly easily implementable workflow named KiQuant for Ki67 LI assessment which showed excellent reproducibility with reference pathologist standard (ICC:0.905) and satisfactory analytical reproducibility (inter-run ICC:0.917; inter-antibody ICC:0.886). KiQuant shows a series of important features that could make standardization of Ki67 interpretation simple and effective. The novelty of our analysis workflow is the ability to fuse the information contained in two different images derived from sequential IHC on the same tissue slide into one single virtual dual staining (VDS) allowing to superimpose epithelial tumor areas, obtained from cytokeratin, and positive cells information, from Ki67 staining. Previous studies using VDS on serial sections for Ki67 LI determination [45,46] found a high correlation between DIA and MS using both TMA and whole slide analyses. However, a high VDS failure rate (24%) was reported [46] due to the unsuccessful alignment of the Ki67-and cytokeratin-

stained serial sections. By using the same slide, our workflow overcomes many of the factors that can cause VDS misalignments, such as differences between cuts, folding, and twisting. As a matter of fact, in our study, none of the cores was excluded due to alignment issues. Additional advantages of KiQuant over conventional VDS protocols are: a) to preserve material for additional biomarkers staining (useful for example for small biopsy samples with scant material), b) to exploit previously Ki67 stained slides through the application of a mask to the original immunostaining or c) to store a smaller number of slides in the laboratories' archives.

In our analysis, we observed that KiQuant returned lower Ki67 LI counts as compared to pathologists' scoring. This was already described in other studies using DIA [46] and it is very likely related to pathologist's underestimation of the negative over the positive tumor nuclei. We found that this imprecision increased with the magnitude of Ki67 LI. This might also explain the significantly higher difference between DIA and MS in HER2+ and TNBC (high Ki67 LI) compared to HR+ (low Ki67 LI) BC subtypes.

Our analyses were conducted using TMA cores. The KiQuant workflow is not significantly different in whole sections. However, as the size of the scored tumor area affected imprecision, we expect that Ki67 heterogeneity and the choice of the scoring area in the whole section may negatively impact on the correlation between DIA and manual scoring in whole sections [21].

Ki67 cut-offs are needed for proper patient stratification and treatment decision. However, there is no absolute agreement regarding cut-off points. It has been recommended that each pathology department should set its most appropriate cut-off points [14]. A 20% cut-off was recommended for distinguishing between Luminal A-like and Luminal B-like tumor types [19]. A recent meta-analysis concluded that a Ki67 level of over 25% is associated with a worse prognosis [47]. In our cohort, we observed a low concordance among observers below the 20% Ki67 LI (ICC: 0.606) and agreement rates between KiQuant and MS within the clinically relevant 14% and 30% cut-off points ranged from 33% to 44% (Fig. 3). In this scenario, automated approaches like KiQuant might improve Ki67 LI reproducibility, specifically around the grey zone area of Ki67 LI of 10–30% where a high level of inter-observer variability has been documented [15,16,48–51]. Importantly, our study found a significant correlation between high Ki67 by KiQuant and worse survival in both the overall cohort and the luminal BC subtype. This prognostic association could be confirmed only for one out of three pathologists' Ki67 assessment. These data, beside showing KiQuant as a accurate method to stratify BC into good and unfavorable prognostic groups, support the value of such immunohistochemical-based test that, if appropriately performed and standardized, may provide an easy and cheap alternative to more expensive genomic-based prognostic assays.

Our study has some limitations. Analyses were conducted using TMA cores instead of whole sections where the much more complex histology and biological heterogeneity may impact on the correlation between DIA and MS. The segmentation using cytokeratin-based mask may not be effective in rarer breast cancer types, such as metaplastic and medullary carcinomas. The performance of our DIA algorithm was tested only on images acquired using a single platform. Lastly, the analysis workflow is not fully automatic, as it requires the supervision (although limited) of a pathologist.

5. Conclusions

To the best of our knowledge, our study is the first one to investigate reproducibility and prognostic potential between standard and DIA Ki67 LI using sequential IHC on a single slide. Our method is technically feasible and potentially useful for both diagnostic and research use as it relies on a slide scanner and an image analysis software which are today available in many pathology departments. KiQuant may improve the standardization of Ki67 by overcoming some of the factors that determine poor reproducibility of Ki67 assessment, such as the selection of the scoring area and manual counting thus increasing the confidence of oncologists toward the use of Ki67 in the clinical setting for treatment recommendations.

Declaration of competing interest

VP has received honoraria from Roche and Sismex; PN has consulted for Bayer, Novartis, MSD, and Targos, and received compensation. The other authors declare no potential conflict of interest.

Acknowledgments

Acknowledgments to the Cellex Foundation for providing research facilities. Work has been realized in the Surgery and Morphological Sciences Doctorate framework of Universitat Autònoma de Barcelona.

Appendix A. Supplementary data

Supplementary data to this article can be found online at https://doi.org/10.1016/j.breast.2020.07.002.

Funding

No relevant funding.

Ethical approval and consent to participate

The protocol of this study was approved by the Vall d'Hebron University Hospital Ethical Committee (PR(AG)76/2018) and all methods were performed in accordance with relevant guidelines and regulations.

The results of this work have been presented at the 31st European Congress of Pathology in Nice, France from 7–September 11, 2019 (ePoster).

References

[1] Gerdes J, Lemke H, Baisch H, Wacker HH, Schwab U, Stein H. Cell cycle analysis of a cell proliferation-associated human nuclear antigen defined by the monoclonal antibody Ki-67. J Immunol 1984;133:1710–5.
[2] Luo G, Hu Y, Zhang Z, Wang P, Luo Z, Lin J, et al. Clinicopathologic significance and prognostic value of Ki-67 expression in patients with gastric cancer: a meta-analysis. Oncotarget 2017;8:50273–83. https://doi.org/10.18632/oncotarget.17305.
[3] de Azambuja E, Cardoso F, de Castro G, Colozza M, Mano MS, Durbecq V, et al. Ki-67 as prognostic marker in early breast cancer: a meta-analysis of published studies involving 12 155 patients. Br J Canc 2007;96:1504–13. https://doi.org/10.1038/sj.bjc.6603756.
[4] Jones RL, Salter J, A'Hern R, Nerurkar A, Parton M, Reis-Filho JS, et al. The prognostic significance of Ki67 before and after neoadjuvant chemotherapy in breast cancer. Breast Canc Res Treat 2009;116:53–68. https://doi.org/10.1007/s10549-008-0081-7.
[5] Zhao W-Y, Xu J, Wang M, Zhang Z-Z, Tu L, Wang C-J, et al. Prognostic value of Ki67 index in gastrointestinal stromal tumors. Int J Clin Exp Pathol 2014;7:2298–304.
[6] Yamaguchi T, Fujimori T, Tomita S, Ichikawa K, Mitomi H, Ohno K, et al. Clinical validation of the gastrointestinal NET grading system: Ki67 index criteria of the WHO 2010 classification is appropriate to predict metastasis or recurrence. Diagn Pathol 2013;8:752. https://doi.org/10.1186/1746-1596-8-65.
[7] Pollack A, DeSilvio M, Khor L-Y, Li R, Al-Saleem TI, Hammond ME, et al. Ki-67 staining is a strong predictor of distant metastasis and mortality for men with prostate cancer treated with radiotherapy plus androgen deprivation: radiation therapy Oncology group trial 92–02. J Clin Oncol 2004;22:2133–40.

https://doi.org/10.1200/JCO.2004.09.150.
[8] Szentkúti G, Dános K, Brauswetter D, Kiszner G, Krenács T, Csákó L, et al. Correlations between prognosis and regional biomarker profiles in head and neck squamous cell carcinomas. Pathol Oncol Res 2015;21:643–50. https://doi.org/10.1007/s12253-014-9869-4.
[9] Pelosi G, Bresaola E, Bogina G, Pasini F, Rodella S, Castelli P, et al. Endocrine tumors of the pancreas: Ki-67 immunoreactivity on paraffin sections is an independent predictor for malignancy: a comparative study with proliferating-cell nuclear antigen and progesterone receptor protein immunostaining, mitotic index, and other clinicopathologic variables. Hum Pathol 1996;27:1124–34.
[10] Yerushalmi R, Woods R, Ravdin PM, Hayes MM, Gelmon KA. Ki67 in breast cancer: prognostic and predictive potential. Lancet Oncol 2010;11:174–83. https://doi.org/10.1016/S1470-2045(09)70262-1.
[11] Viale G, Giobbie-Hurder A, Regan MM, Coates AS, Mastropasqua MG, Dell'Orto P, et al. Prognostic and predictive value of centrally reviewed ki-67 labeling index in postmenopausal women with endocrine-responsive breast cancer: results from breast international group trial 1-98 comparing adjuvant tamoxifen with letrozole. J Clin Oncol 2008;26:5569–75. https://doi.org/10.1200/JCO.2008.17.0829.
[12] Kurozumi SI, Yamaguchi Y, Matsumoto H, Kurosumi M, Hayashi S, Fujii T, et al. Utility of Ki67 labeling index, cyclin D1 expression, and ER-activity level in postmenopausal ER-positive and HER2-negative breast cancer with neoadjuvant chemo-endocrine therapy. 2019. https://doi.org/10.1371/journal.pone.0217279.
[13] Ács B, Zámbó V, Vízkeleti L, Szász AM, Madaras L, Szentmártoni G, et al. Ki-67 as a controversial predictive and prognostic marker in breast cancer patients treated with neoadjuvant chemotherapy. Diagn Pathol 2017;12:20. https://doi.org/10.1186/s13000-017-0608-5.
[14] Dowsett M, Nielsen TO, A'Hern R, Bartlett J, Coombes RC, Cuzick J, et al. Assessment of Ki67 in breast cancer: recommendations from the international Ki67 in breast cancer working group. JNCI J Natl Cancer Inst 2011;103:1656–64. https://doi.org/10.1093/jnci/djr393.
[15] Polley M-YC, Leung SCY, Gao D, Mastropasqua MG, Zabaglo LA, Bartlett JMS, et al. An international study to increase concordance in Ki67 scoring. Mod Pathol 2015;28:778–86. https://doi.org/10.1038/modpathol.2015.38.
[16] Shui R, Yu B, Bi R, Yang F, Yang W. An interobserver reproducibility analysis of Ki67 visual assessment in breast cancer. PloS One 2015;10:e0125131. https://doi.org/10.1371/journal.pone.0125131.
[17] Christgen M, von Ahsen S, Christgen H, Länger F, Kreipe H. The region-of-interest size impacts on Ki67 quantification by computer-assisted image analysis in breast cancer. Hum Pathol 2015;46:1341–9. https://doi.org/10.1016/j.humpath.2015.05.016.
[18] Leung SCY, Nielsen TO, Zabaglo LA, Arun I, Badve SS, Bane AL, et al. Analytical validation of a standardised scoring protocol for Ki67 immunohistochemistry on breast cancer excision whole sections: an international multicentre collaboration. Histopathology 2019;75:225–35. https://doi.org/10.1111/his.13880.
[19] Goldhirsch A, Winer EP, Coates AS, Gelber RD, Piccart-Gebhart M, Thürlimann B, et al. Personalizing the treatment of women with early breast cancer: highlights of the st gallen international expert consensus on the primary therapy of early breast cancer 2013. Ann Oncol 2013;24:2206–23. https://doi.org/10.1093/annonc/mdt303.
[20] Falck A-K, Fernö M, Bendahl P-O, Rydén L. St Gallen molecular subtypes in primary breast cancer and matched lymph node metastases - aspects on distribution and prognosis for patients with luminal A tumours: results from a prospective randomised trial. BMC Canc 2013;13:558. https://doi.org/10.1186/1471-2407-13-558.
[21] Focke CM, van Diest PJ, Decker T. St Gallen 2015 subtyping of luminal breast cancers: impact of different Ki67-based proliferation assessment methods. Breast Canc Res Treat 2016;159:257–63. https://doi.org/10.1007/s10549-016-3950-5.
[22] Dowsett M, Cuzick J, Wale C, Forbes J, Mallon EA, Salter J, et al. Prediction of risk of distant recurrence using the 21-gene recurrence score in node-negative and node-positive postmenopausal patients with breast cancer treated with anastrozole or tamoxifen: a TransATAC study. J Clin Oncol 2010;28:1829–34. https://doi.org/10.1200/JCO.2009.24.4798.
[23] Sestak I, Cuzick J, Dowsett M, Lopez-Knowles E, Filipits M, Dubsky P, et al. Prediction of late distant recurrence after 5 years of endocrine treatment: a combined analysis of patients from the Austrian breast and colorectal cancer study group 8 and Arimidex, Tamoxifen Alone or in combination randomized trials using the PAM50 risk of recurrence score. J Clin Oncol 2015;33:916–22. https://doi.org/10.1200/JCO.2014.55.6894.
[24] Albain KS, Barlow WE, Shak S, Hortobagyi GN, Livingston RB, Yeh IT, et al. Prognostic and predictive value of the 21-gene recurrence score assay in postmenopausal women with node-positive, oestrogen-receptor-positive breast cancer on chemotherapy: a retrospective analysis of a randomised trial. Lancet Oncol 2010;11:55–65. https://doi.org/10.1016/S1470-2045(09)70314-6.
[25] Ács B, Madaras L, Kovács KA, Micsik T, Tőkés A-M, Győrffy B, et al. Reproducibility and prognostic potential of ki-67 proliferation index when comparing digital-image analysis with standard semi-quantitative evaluation in breast cancer. Pathol Oncol Res 2018;24:115–27. https://doi.org/10.1007/s12253-017-0220-8.
[26] Stålhammar G, Robertson S, Wedlund L, Lippert M, Rantalainen M, Bergh J, et al. Digital image analysis of Ki67 in hot spots is superior to both manual Ki67 and mitotic counts in breast cancer. Histopathology 2018;72:974–89. https://doi.org/10.1111/his.13452.
[27] Stålhammar G, Fuentes Martinez N, Lippert M, Tobin NP, Mølholm I, Kis L, et al. Digital image analysis outperforms manual biomarker assessment in breast cancer. Mod Pathol 2016;29:318–29. https://doi.org/10.1038/modpathol.2016.34.
[28] Klauschen F, Wienert S, Schmitt WD, Loibl S, Gerber B, Blohmer J-U, et al. Standardized Ki67 diagnostics using automated scoring–clinical validation in the GeparTrio breast cancer study. Clin Canc Res 2015;21:3651–7. https://doi.org/10.1158/1078-0432.CCR-14-1283.
[29] Zhong F, Bi R, Yu B, Yang F, Yang W, Shui R. A Comparison of visual assessment and automated digital image analysis of Ki67 labeling index in breast cancer. PloS One 2016;11:e0150505. https://doi.org/10.1371/journal.pone.0150505.
[30] Koopman T, Buikema HJ, Hollema H, de Bock GH, van der Vegt B. Digital image analysis of Ki67 proliferation index in breast cancer using virtual dual staining on whole tissue sections: clinical validation and inter-platform agreement. Breast Canc Res Treat 2018;169:33–42. https://doi.org/10.1007/s10549-018-4669-2.
[31] Røge R, Riber-Hansen R, Nielsen S, Vyberg M. Proliferation assessment in breast carcinomas using digital image analysis based on virtual Ki67/cytokeratin double staining. Breast Canc Res Treat 2016;158:11–9. https://doi.org/10.1007/s10549-016-3852-6.
[32] Joseph J, Roudier MP, Narayanan PL, Augulis R, Ros VR, Pritchard A, et al. Proliferation Tumour Marker Network (PTM-NET) for the identification of tumour region in Ki67 stained breast cancer whole slide images. Sci Rep 2019;9:12845. https://doi.org/10.1038/s41598-019-49139-4.
[33] Landis JR, Koch GG. The measurement of observer agreement for categorical data. Biometrics 1977;33:159–74.
[34] Stuart-Harris R, Caldas C, Pinder SE, Pharoah P. Proliferation markers and survival in early breast cancer: a systematic review and meta-analysis of 85 studies in 32,825 patients. Breast 2008;17:323–34. https://doi.org/10.1016/j.breast.2008.02.002.
[35] Criscitiello C, Disalvatore D, De Laurentiis M, Gelao L, Fumagalli L, Locatelli M, et al. High Ki-67 score is indicative of a greater benefit from adjuvant chemotherapy when added to endocrine therapy in Luminal B HER2 negative and node-positive breast cancer. Breast 2014;23:69–75. https://doi.org/10.1016/j.breast.2013.11.007.
[36] Brown JR, DiGiovanna MP, Killelea B, Lannin DR, Rimm DL. Quantitative assessment Ki-67 score for prediction of response to neoadjuvant chemotherapy in breast cancer. Lab Invest 2014;94:98–106. https://doi.org/10.1038/labinvest.2013.128.
[37] Ács B, Zámbó V, Vízkeleti L, Szász AM, Madaras L, Szentmártoni G, et al. Ki-67 as a controversial predictive and prognostic marker in breast cancer patients treated with neoadjuvant chemotherapy. Diagn Pathol 2017;12:20. https://doi.org/10.1186/s13000-017-0608-5.
[38] Cuzick J, Dowsett M, Pineda S, Wale C, Salter J, Quinn E, et al. Prognostic value of a combined estrogen receptor, progesterone receptor, Ki-67, and human epidermal growth factor. J Clin Oncol 2011;29:4273–8. https://doi.org/10.1200/JCO.2010.31.2835.
[39] Polley M-YC, Leung SCY, McShane LM, Gao D, Hugh JC, Mastropasqua MG, et al. An international Ki67 reproducibility study. JNCI J Natl Cancer Inst 2013;105:1897–906. https://doi.org/10.1093/jnci/djt306.
[40] Dowsett M, Nielsen TO, A'Hern R, Bartlett J, Coombes RC, Cuzick J, et al. Assessment of Ki67 in breast cancer: recommendations from the international Ki67 in breast cancer working group. JNCI J Natl Cancer Inst 2011;103:1656–64. https://doi.org/10.1093/jnci/djr393.
[41] Senkus E, Kyriakides S, Ohno S, Penault-Llorca F, Poortmans P, Rutgers E, et al. Primary breast cancer: ESMO Clinical Practice Guidelines for diagnosis, treatment and follow-up. Ann Oncol 2015;26. https://doi.org/10.1093/annonc/mdv298. v8–30.
[42] Bankhead P, Loughrey MB, Fernández JA, Dombrowski Y, McArt DG, Dunne PD, et al. QuPath: open source software for digital pathology image analysis. Sci Rep 2017;7:16878. https://doi.org/10.1038/s41598-017-17204-5.
[43] Ruifrok AC, Johnston DA. Quantification of histochemical staining by color deconvolution, vol. 23; 2001.
[44] Acs B, Pelekanou V, Bai Y, Martinez-Morilla S, Toki M, Leung SCY, et al. Ki67 reproducibility using digital image analysis: an inter-platform and inter-operator study. Lab Invest 2019;99:107–17. https://doi.org/10.1038/s41374-018-0123-7.
[45] Røge R, Riber-Hansen R, Nielsen S, Vyberg M. Proliferation assessment in breast carcinomas using digital image analysis based on virtual Ki67/cytokeratin double staining. Breast Canc Res Treat 2016;158:11–9. https://doi.org/10.1007/s10549-016-3852-6.
[46] Koopman T, Buikema HJ, Hollema H, de Bock GH, van der Vegt B. Digital image analysis of Ki67 proliferation index in breast cancer using virtual dual staining on whole tissue sections: clinical validation and inter-platform agreement. Breast Canc Res Treat 2018;169:33–42. https://doi.org/10.1007/s10549-018-4669-2.
[47] Petrelli F, Viale G, Cabiddu M, Barni S. Prognostic value of different cut-off levels of Ki-67 in breast cancer: a systematic review and meta-analysis of 64,196 patients. Breast Canc Res Treat 2015;153:477–91. https://doi.org/10.1007/s10549-015-3559-0.
[48] Varga Z, Diebold J, Dommann-Scherrer C, Frick H, Kaup D, Noske A, et al. How reliable is ki-67 immunohistochemistry in grade 2 breast carcinomas? A qa

study of the Swiss working group of breast- and gynecopathologists. PloS One 2012;7:e37379. https://doi.org/10.1371/journal.pone.0037379.
[49] Cserni G, Vörös A, Liepniece-Karele I, Bianchi S, Vezzosi V, Grabau D, et al. Distribution pattern of the Ki67 labelling index in breast cancer and its implications for choosing cut-off values. Breast 2014;23:259–63. https://doi.org/10.1016/j.breast.2014.02.003.
[50] Laenkholm A-V, Grabau D, Møller Talman M-L, Balslev E, Bak Jylling AM, Tabor TP, et al. An inter-observer Ki67 reproducibility study applying two different assessment methods: on behalf of the Danish Scientific Committee of Pathology, Danish breast cancer cooperative group (DBCG). Acta Oncol (Madr) 2018;57:83–9. https://doi.org/10.1080/0284186X.2017.1404127.
[51] Hida AI, Oshiro Y, Inoue H, Kawaguchi H, Yamashita N, Moriya T. Visual assessment of Ki67 at a glance is an easy method to exclude many luminal-type breast cancers from counting 1000 cells. Breast Cancer 2015;22:129–34. https://doi.org/10.1007/s12282-013-0460-8.